Comparative Analysis of Linear and Nonlinear Attitude Control Strategies for a CubeSat

Joaquín Pozo
Engineering Department
Pontifical Catholic University of Peru
Lima, Peru
joaquin.pozo@pucp.edu.pe

Franchesco Guillermo
Engineering Department
Pontifical Catholic University of Peru
Lima, Peru
a20221148@pucp.edu.pe

***Abstract*—CubeSats have become a widely adopted platform for low-cost space missions, requiring reliable attitude control systems to achieve accurate pointing and tracking objectives under limited actuation capabilities. The inherent nonlinear rotational dynamics of spacecraft and the presence of physical constraints pose significant challenges for attitude control design, particularly in small satellite platforms.**

This paper presents a comparative analysis of linear and nonlinear attitude tracking control strategies applied to a CubeSat platform based on the skCube satellite. A Lyapunov-based nonlinear controller and a sliding mode controller are designed using the full nonlinear attitude dynamics, while a linear quadratic regulator (LQR) is implemented as a baseline controller based on a linearized model. The controllers are evaluated through numerical simulations under identical attitude tracking scenarios, including actuator saturation and external disturbance torques.

The comparative study assesses tracking accuracy, angular velocity regulation, and control effort, highlighting the trade-offs between linear and nonlinear control approaches for CubeSat attitude tracking applications. The results provide insights into the suitability of each control strategy for small satellite missions subject to nonlinear dynamics and actuation limitations.

***Index Terms*—CubeSat, Spacecraft Attitude Dynamics, Lyapunov Function, PD Controller, Sliding Mode Control.**

I. Introduction

CubeSats are a standardized, modular, and low-cost spacecraft platform, that represents a class of functional picosatellites. This architecture provides accessible space capabilities to universities, research institutions, and private organizations by significantly reducing development and launch costs [1]. CubeSats now support a broad range of operational applications, including Earth observation, communications, and in-orbit technology demonstration. This versatility has driven sustained global growth, as evidenced by the deployment of over one thousand CubeSats worldwide over the past two decades [5].

CubeSats must regulate their orientation across different operational phases, a function performed by the Attitude Determination and Control System (ADCS). From a control perspective, the ADCS is responsible for post-deployment stabilization, detumbling maneuvers, and achieving accurate attitude pointing or tracking as required by the mission. However, attitude control system design are challenged by the nonlinear nature of spacecraft rotational dynamics and external disturbances, while being further constrained by limited and often underactuated actuation architectures, which impose strict physical bounds on the achievable control response.

To address the challenges of CubeSat attitude control, a variety of linear and nonlinear control strategies have been reported in the literature. Said et al. [4] developed an integrated simulation framework employing a two-stage control strategy, combining a B-Dot controller for detumbling with a PD controller for attitude reorientation and nadir tracking, demonstrating convergence within mission-relevant time frames. More advanced linear approaches have also been explored; for instance, Mamarasulov et al. [3] implemented a model predictive control (MPC) scheme for trajectory tracking, incorporating a time-varying linear model and an extended Kalman filter, and reported improved performance over an LQR controller, particularly in terms of smoother control action and explicit handling of actuation constraints. Nonlinear control techniques have likewise been investigated, as shown by Cortes et al. [2], who designed Lyapunov-based and sliding mode controllers for CubeSat attitude maneuvers involving solar pointing, nadir pointing, and active tracking. Their comparative analysis highlighted the superior tracking accuracy of sliding mode control, albeit at the cost of increased control effort. Despite these contributions, a systematic comparison of linear and nonlinear control strategies under a unified nonlinear model and identical tracking scenarios remains limited, motivating the need for further comparative analysis.

In this paper, a comparative analysis of attitude control strategies for the first Slovak satellite, designated skCube. A Lyapunov-based controller and a sliding mode controller are designed based on the nonlinear rotational dynamics of the spacecraft, while a linear quadratic regulator (LQR) is implemented as a baseline controller using a linearized model. The controllers are evaluated under identical attitude tracking scenarios through numerical simulations, allowing a consistent assessment of their tracking performance, control effort, and robustness characteristics. The results provide insight into the advantages and limitations of linear and nonlinear control approaches when applied to CubeSat attitude tracking problems.

II. System Modeling

When dealing with the analysis of spacecraft rotational motion, the definition of appropriate reference coordinate

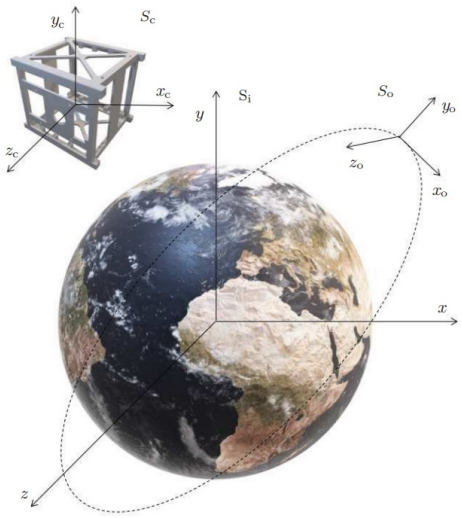

Fig. 1. Illustration of different reference frames

systems is essential to accurately describe the attitude and angular motion of the vehicle. In general, spacecraft dynamics are formulated with respect to an inertial reference frame, denoted as $\mathcal{F}_I$, which is assumed to be non-accelerating and serves as a fixed reference for attitude description. In addition, a body-fixed reference frame, denoted as $\mathcal{F}_B$, is introduced and rigidly attached to the spacecraft. The body frame is aligned with the principal axes of inertia and rotates together with the spacecraft, making it suitable for expressing angular velocities, inertia properties, and control torques.

The relative orientation between the inertial frame $\mathcal{F}_I$ and the body-fixed frame $\mathcal{F}_B$ fully characterizes the spacecraft attitude and enables a compact formulation of both kinematic and dynamic equations. The reference frames considered in this work, along with their relative orientation, are illustrated in Fig.1 and form the basis for the attitude modeling and control design developed in the following sections.

A. Attitude dynamics

The spacecraft rotational dynamics are described by Euler's equation for a rigid body, expressed in the body-fixed reference frame $\mathcal{F}_B$:

$$I_b\dot{\boldsymbol{\omega}} = -\boldsymbol{\omega} \times (I_b\boldsymbol{\omega}) + \boldsymbol{\tau}, \tag{1}$$

where $I_b \in \mathbb{R}^{3\times3}$ denotes the spacecraft inertia matrix expressed in $\mathcal{F}_B$, $\boldsymbol{\omega} \in \mathbb{R}^3$ is the angular velocity of the spacecraft, and $\boldsymbol{\tau} \in \mathbb{R}^3$ represents the control torque applied to the spacecraft.

The inertia matrix is assumed to be constant and diagonal, corresponding to a rigid spacecraft whose body-fixed axes are aligned with the principal axes of inertia. The nonlinear term $\boldsymbol{\omega} \times (I_b\boldsymbol{\omega})$ captures the coupling between the angular velocity components and plays a key role in the nonlinear behavior of the attitude dynamics.

B. Relative Kinematics

The relative orientation between the inertial reference frame $\mathcal{F}_I$ and the body-fixed frame $\mathcal{F}_B$ is described using a unit quaternion representation. The quaternion is defined as

$$q = \begin{bmatrix} q_0 & q_1 & q_2 & q_3 \end{bmatrix}^T, \tag{2}$$

where q_0 denotes the scalar component and $\mathbf{q}_v = [q_1\ q_2\ q_3]^T$ represents the vector part. The quaternion representation is adopted due to its global validity and the absence of singularities, making it suitable for describing large-angle spacecraft rotations. The unit-norm constraint on the quaternion is assumed to be satisfied throughout the motion.

The time evolution of the quaternion is governed by the relative kinematic equation

$$\dot{q} = \frac{1}{2}\,\Omega(\boldsymbol{\omega})\,q, \tag{3}$$

where $\boldsymbol{\omega} \in \mathbb{R}^3$ is the angular velocity of the spacecraft expressed in the body-fixed frame $\mathcal{F}_B$. The matrix $\Omega(\boldsymbol{\omega}) \in \mathbb{R}^{4\times4}$ is defined as

$$\Omega(\boldsymbol{\omega}) = \begin{bmatrix} 0 & -\omega_x & -\omega_y & -\omega_z \\ \omega_x & 0 & \omega_z & -\omega_y \\ \omega_y & -\omega_z & 0 & \omega_x \\ \omega_z & \omega_y & -\omega_x & 0 \end{bmatrix}. \tag{4}$$

C. Nonlinear Model

By combining the rotational dynamics and the relative kinematics, the nonlinear attitude motion of the spacecraft can be expressed in state-space form. The state vector is defined as

$$x = \begin{bmatrix} q^T & \boldsymbol{\omega}^T \end{bmatrix}^T \in \mathbb{R}^7, \tag{5}$$

where $q \in \mathbb{R}^4$ is the unit quaternion representing the spacecraft attitude and $\boldsymbol{\omega} \in \mathbb{R}^3$ is the angular velocity expressed in the body-fixed frame $\mathcal{F}_B$. The nonlinear state equations are given by

$$\begin{aligned} \dot{q} &= \frac{1}{2}\,\Omega(\boldsymbol{\omega})\,q, \\ \dot{\boldsymbol{\omega}} &= I_b^{-1}\left(-\boldsymbol{\omega} \times (I_b\boldsymbol{\omega}) + \boldsymbol{\tau} + \boldsymbol{\tau}_d\right), \end{aligned} \tag{6}$$

where $\boldsymbol{\tau} \in \mathbb{R}^3$ denotes the control torque and $\boldsymbol{\tau}_d \in \mathbb{R}^3$ represents external disturbance torques.

By substituting the state vector $\boldsymbol{x} = [\eta\ q_1\ q_2\ q_3\ \omega_1\ \omega_2\ \omega_3]^T$ into (6) and assuming that both the spacecraft attitude and angular velocity are available for measurement, the following continuous-time nonlinear state-space model is obtained:

$$\dot{\boldsymbol{x}} = \begin{bmatrix} -\frac{1}{2}\left(x_2x_5 + x_3x_6 + x_4x_7\right) \\ \frac{1}{2}\left(x_1x_5 + x_3x_7 - x_4x_6\right) \\ \frac{1}{2}\left(x_1x_6 - x_2x_7 + x_4x_5\right) \\ \frac{1}{2}\left(x_1x_7 + x_2x_6 - x_3x_5\right) \\ \frac{1}{I_x}\left(u_1 + (I_y - I_z)x_6x_7\right) \\ \frac{1}{I_y}\left(u_2 + (I_z - I_x)x_5x_7\right) \\ \frac{1}{I_z}\left(u_3 + (I_x - I_y)x_5x_6\right) \end{bmatrix}, \qquad \boldsymbol{y} = \begin{bmatrix} x_1 \\ x_2 \\ x_3 \\ x_4 \\ x_5 \\ x_6 \\ x_7 \end{bmatrix} \tag{7}$$

where $\boldsymbol{u} = [u_1\ u_2\ u_3]^T$ denotes the applied control torque vector.

D. Linearized Model

In order to enable the application of linear control techniques, the nonlinear spacecraft attitude dynamics are linearized about a nominal operating point. The resulting linearized model provides a local approximation of the system behavior in the vicinity of the selected equilibrium and is commonly employed for the synthesis of linear feedback control laws.

The linearization is carried out around an equilibrium corresponding to zero angular velocity and small attitude errors, defined by

$$\boldsymbol{x}_e = \begin{bmatrix} \mathbf{0}_{3\times1} \\ \mathbf{0}_{3\times1} \end{bmatrix}, \qquad \boldsymbol{u}_e = \mathbf{0}_{3\times1}, \tag{8}$$

which represents a spacecraft aligned with the reference attitude and at rest.

Let $\delta\boldsymbol{x} = \boldsymbol{x} - \boldsymbol{x}_e$ and $\delta\boldsymbol{u} = \boldsymbol{u} - \boldsymbol{u}_e$ denote small perturbations around the equilibrium point. Under the assumption of small attitude deviations, the nonlinear dynamics can be approximated by the linear time-invariant model

$$\delta\dot{\boldsymbol{x}} = \boldsymbol{A}\,\delta\boldsymbol{x} + \boldsymbol{B}\,\delta\boldsymbol{u}, \tag{9}$$

where the system matrices are given by

$$\boldsymbol{A} = \begin{bmatrix} \mathbf{0}_{3\times3} & \frac{1}{2}\boldsymbol{I}_{3\times3} \\ \mathbf{0}_{3\times3} & \mathbf{0}_{3\times3} \end{bmatrix}, \qquad \boldsymbol{B} = \begin{bmatrix} \mathbf{0}_{3\times3} \\ \operatorname{diag}\left(\frac{1}{I_x}, \frac{1}{I_y}, \frac{1}{I_z}\right) \end{bmatrix}. \tag{10}$$

This linearized representation neglects higher-order nonlinear terms and external disturbances, and is therefore valid only in a local neighborhood of the equilibrium point. Nevertheless, it provides a useful framework for the design and evaluation of linear attitude control strategies.

III. Controller design

In this section, three attitude control strategies are presented based on the spacecraft system equations. A simplified block diagram of the control system architecture is shown in Fig. 2. The subsequent subsections present the design methodology for each of these controllers and their respective performance evaluations.

A. Lyapunov-Based Control (LBC)

Lyapunov-based control provides a systematic framework for the design of nonlinear feedback laws by ensuring closed-loop stability through the construction of an appropriate Lyapunov function. The central idea is to select a positive definite scalar function of the system states whose time derivative along system trajectories is negative definite, thereby guaranteeing asymptotic stability without requiring linearization of the dynamics.

In this work, a Lyapunov candidate function is chosen as

$$V(\boldsymbol{x}) = \frac{1}{2}\,\boldsymbol{\omega}^T\boldsymbol{I}\boldsymbol{\omega} + k\left(\boldsymbol{q}_v^T\boldsymbol{q}_v + (1-q_0)^2\right), \tag{11}$$

where $\boldsymbol{q}_v = [q_1 \;\; q_2 \;\; q_3]^T$ denotes the vector part of the quaternion, q_0 is its scalar component, $\boldsymbol{\omega}$ is the angular velocity vector, $\boldsymbol{I} = \operatorname{diag}(I_x, I_y, I_z)$ is the inertia matrix, and $k > 0$ is a design parameter. The first term represents the rotational kinetic energy, while the second term penalizes attitude errors. The function V is positive definite with respect to the equilibrium $(\boldsymbol{q}, \boldsymbol{\omega}) = ([1\;0\;0\;0]^T, \mathbf{0})$.

Taking the time derivative of V along the trajectories of the nonlinear system yields

$$\dot{V} = \boldsymbol{\omega}^T\boldsymbol{\tau} + k\,\boldsymbol{q}_v^T\boldsymbol{\omega}. \tag{12}$$

A proportional-derivative (PD) control law is selected as

$$\boldsymbol{\tau} = -\boldsymbol{K}_p\,\boldsymbol{q}_v - \boldsymbol{K}_d\,\boldsymbol{\omega}, \tag{13}$$

where $\boldsymbol{K}_p = k\,\boldsymbol{I}_{3\times3}$ and $\boldsymbol{K}_d = \operatorname{diag}(k_{d1}, k_{d2}, k_{d3})$ are positive definite gain matrices.

Substituting the control law (13) into (12) results in

$$\dot{V} = -\boldsymbol{\omega}^T\boldsymbol{K}_d\boldsymbol{\omega}, \tag{14}$$

which is negative definite for $\boldsymbol{\omega} \neq \mathbf{0}$. Therefore, $\dot{V} < 0$ for all nonzero angular velocities, and $\dot{V} = 0$ only when $\boldsymbol{\omega} = \mathbf{0}$.

By invoking LaSalle's invariance principle, it follows that the closed-loop system trajectories converge asymptotically to the largest invariant set contained in $\{\dot{V} = 0\}$, which corresponds to the desired equilibrium attitude. Hence, the proposed Lyapunov-based control law guarantees global asymptotic stability of the spacecraft attitude.

B. Sliding Mode Control (SMC)

A sliding mode control strategy is proposed to achieve robust tracking of a time-varying attitude reference $x_d(t) = [q_d^T(t), \omega_d^T(t)]^T$ in the presence of model uncertainties and external disturbances τ_d. [6], [7]. The controller design follows a two-step procedure: the construction of a stabilizing sliding surface using the regular form transformation, and the synthesis of a composite control law combining feedforward compensation, linear stabilization, and a robust nonlinear term based on the unit-vector approach.

1) Sliding Surface Design: Let the tracking error be defined as $\tilde{x} = x - x_d$. Considering the linearized tracking error dynamics around the operating point,

$$\dot{\tilde{x}} = A\tilde{x} + B\tilde{u}, \tag{15}$$

where $\tilde{u} = u - u_{ff}$ represents the control input acting on the error system. A coordinate transformation $z = T_r\tilde{x}$ is introduced, where the orthogonal matrix T_r is obtained from the full QR decomposition of the input matrix B. This transformation brings the system into regular form, separating

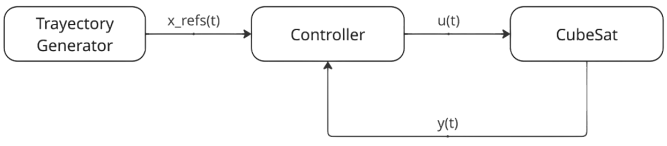

Fig. 2. Simplified block diagram of proposed attitude control system

the undriven dynamics z_1 from the directly actuated dynamics z_2 [6].

The sliding surface $\sigma \in \mathbb{R}^3$ is defined as

$$\sigma = S\tilde{x} = S_2 \begin{bmatrix} M & I_3 \end{bmatrix} T_r \tilde{x}, \tag{16}$$

where S_2 is selected such that $SB = I_3$, ensuring decoupled switching dynamics, and the matrix M is designed via pole placement to assign the eigenvalues of the reduced-order sliding dynamics. Consequently, when the system reaches the sliding surface ($\sigma = 0$), the attitude tracking error converges asymptotically to zero with the desired transient performance.

2) Control Law: To guarantee finite-time reachability of the sliding surface and accurate tracking of the reference trajectory, the following composite control law is proposed:

$$u = u_{ff} + u_l + u_{rn}. \tag{17}$$

The feedforward term u_{ff} compensates for the nominal rotational dynamics associated with the desired motion and is derived from the inverse rigid-body dynamics, as commonly adopted in nonlinear attitude control schemes [8], [7],

$$u_{ff} = I_b \dot{\omega}_d + \omega \times (I_b \omega), \tag{18}$$

where I_b denotes the spacecraft inertia matrix and ω is the measured angular velocity.

The linear stabilizing term is defined as

$$u_l = -(SB)^{-1} SA\tilde{x} + (SB)^{-1} \Phi \sigma, \tag{19}$$

where Φ is a Hurwitz matrix that governs the convergence rate of the sliding variable during the reaching phase.

Finally, robustness against bounded matched uncertainties and external disturbances is ensured through the nonlinear unit-vector term

$$u_{rn} = -\rho (SB)^{-1} \frac{\sigma}{\|\sigma\| + \delta}, \tag{20}$$

where $\rho > 0$ is a switching gain chosen to dominate the uncertainty bounds, and $\delta > 0$ is a small regularization constant introduced to mitigate chattering effects in the vicinity of the sliding surface.

C. Linear Quadratic Regulator (LQR)

The objective of the LQR is to compute a state-feedback control law that minimizes a quadratic performance index while balancing state regulation performance and control effort.

Considering the linearized spacecraft model expressed in (9) the LQR problem consists of minimizing the cost function

$$J = \int_0^\infty \left(\delta \boldsymbol{x}^T \boldsymbol{Q}\, \delta \boldsymbol{x} + \delta \boldsymbol{u}^T \boldsymbol{R}\, \delta \boldsymbol{u} \right) dt, \tag{21}$$

where $\boldsymbol{Q} \succeq 0$ and $\boldsymbol{R} \succ 0$ are weighting matrices that penalize state deviations and control effort, respectively.

The optimal control law that minimizes the performance index is given by the linear state-feedback

$$\delta \boldsymbol{u} = -\boldsymbol{K}\, \delta \boldsymbol{x}, \tag{22}$$

where the gain matrix $\boldsymbol{K}$ is obtained by solving the algebraic Riccati equation (ARE).

IV. Simulation Results

This section presents a comparative numerical evaluation of the proposed attitude control strategies. The CubeSat is simulated in a circular orbit at an altitude of 500 km with an inclination of 90°. The initial state is defined as $x_0 = [q_0^T \ \boldsymbol{\omega}_0^T]^T$, where both the initial attitude and angular velocity are nonzero. The executive task of the controller is to maintain the spacecraft attitude within a prescribed domain of orientations during an observation phase.

The reference attitude trajectory is generated in the nadir-pointing frame by drawing a circular path with a radius of π, resulting in a set of 42 reference orientations uniformly distributed around the trajectory. The initial attitude corresponds to both the first and last reference orientation, ensuring trajectory continuity. The satellite is assumed to maintain each desired orientation for a duration of 10 seconds, representing the time required to perform onboard observation tasks.

An overview of the simulation model parameters, including spacecraft mass properties, initial conditions, disturbance torques, and control design bounds, is provided in Table I.

The external disturbance torque is modeled as a bounded, time-varying signal acting equally on all body axes and is defined as

$$\boldsymbol{\tau}_d(t) = \begin{cases} \mathbf{0}, & t < 200 \wedge t >= 302 \text{ s}, \\ 4.7 \times 10^{-6} \sin\left(\frac{\pi}{4} t\right) \mathbf{1}, & 200 \le t < 300 \text{ s}, \\ 0.5 \times 10^{-4} \mathbf{1}, & 300 \le t < 302 \text{ s}, \end{cases} \tag{23}$$

where $\mathbf{1} = [1\ 1\ 1]^T$.

For the linear quadratic controller, the weighting matrices $\boldsymbol{Q}$ and $\boldsymbol{R}$ are selected following Bryson's rule. Each state and control input is normalized with respect to its maximum admissible value, defined by the attitude and angular velocity bounds reported in Table I. This selection ensures a balanced trade-off between tracking accuracy and control effort while maintaining consistency with actuator limitations.

TABLE I
Simulation Model Parameters

Parameter	Symbol	Value	Unit
Spacecraft mass	m	1.056	kg
Moment of inertia (x-axis)	I_x	319×10^{-6}	kg·m^2
Moment of inertia (y-axis)	I_y	420×10^{-6}	kg·m^2
Moment of inertia (z-axis)	I_z	521×10^{-6}	kg·m^2
Initial attitude (quaternion)	q_0	$[0.14, 0.3, -0.2, -0.8]^T$	
Initial angular velocity	$\boldsymbol{\omega}_0$	$[0.2, -0.3, 0.6]^T$	
Disturbance torque profile	$\boldsymbol{\tau}_d(t)$	Bounded time-varying	N·m
Control torque limit	$\boldsymbol{\tau}_{\max}$	$\pm 5 \times 10^{-4}$	N·m
Maximum attitude error	$q_{v,\max}$	0.6	deg
Maximum angular velocity	$\omega_{\max}$	1	deg/s

A. Controllers Under Comparison

In this study, three different attitude control strategies are evaluated and compared based on their tracking performance and energy consumption:

- **Lyapunov-Based Control (LBC):** This approach employs a Lyapunov function to ensure stability of the attitude tracking error dynamics. It is a well-known method for nonlinear systems and is often used for stabilizing systems with uncertain dynamics.
- **Sliding Mode Control (SMC):** The sliding mode controller is designed to handle system uncertainties and disturbances by forcing the system states to slide along a predefined surface in the state space. SMC is known for its robustness but can suffer from chattering, which is mitigated by the use of a feedforward term in the proposed method.
- **Linear Quadratic Regulator (LQR):** LQR is a widely used linear control strategy that optimizes a cost function based on the system's state and control effort. Although it assumes a linear model, it provides a good benchmark for performance comparison and is often employed in systems with relatively predictable dynamics.

All controllers are implemented under the same simulation conditions and are evaluated based on the following criteria: tracking accuracy, control effort, and robustness to external disturbances.

B. Attitude Tracking Performance

The attitude tracking performance of the three control strategies is evaluated by comparing the tracking errors of the desired attitude trajectory. The tracking accuracy of each controller is assessed by computing the Integral of Squared Error (ISE) for the quaternion error.

Figures 3, 4, and 5 show the attitude tracking results for the LQR, SMC, and LBC controllers, respectively. In these figures, the actual quaternion trajectory is compared to the reference trajectory, and the tracking error is plotted over time. The quaternion error for each controller is calculated as the difference between the current attitude and the reference attitude, where the vector part of the quaternion error is used as the performance metric. Figures 6, 7, and 8 show control effort of the system during the cubesat operation.

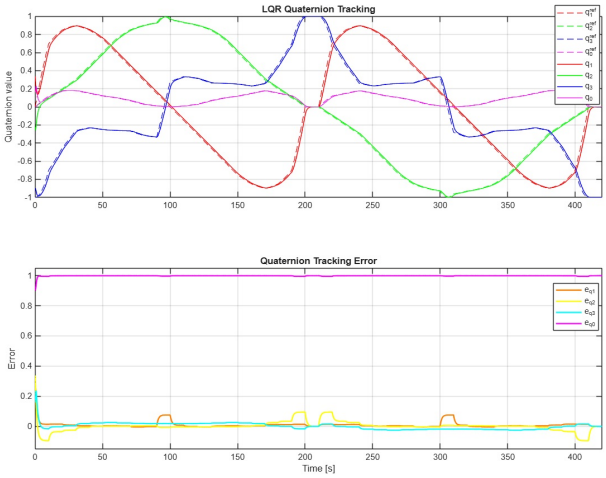

Fig. 3. Attitude Tracking using LQR controller

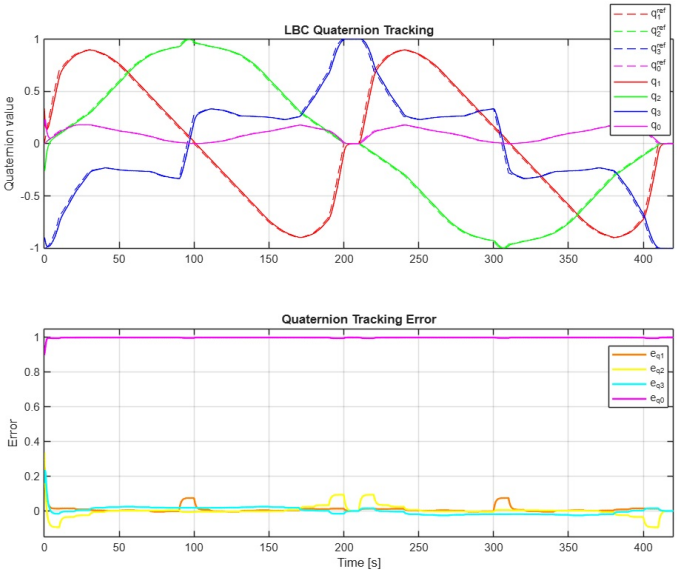

Fig. 4. Attitude Tracking using Lyapunov-Based Control

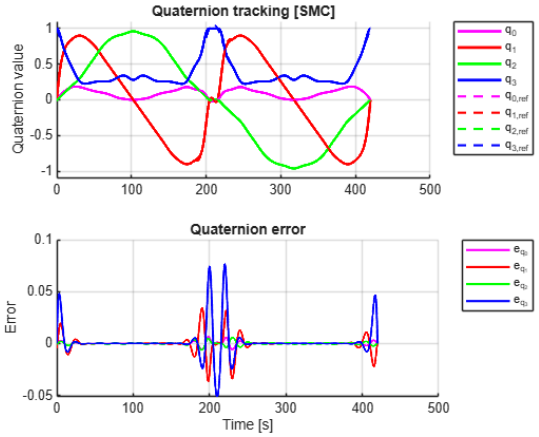

Fig. 5. Attitude Tracking using SMC

C. Performance Indices Comparison

To quantitatively compare the control strategies, the Integral of Squared Error (ISE) is employed as a tracking performance metric, defined as

$$\text{ISE} = \int_0^T \|q_v(t) - q_{v,d}(t)\|^2 \, dt. \tag{24}$$

TABLE II
PERFORMANCE INDICES COMPARISON

Controller	ISE	Energy Index	Max Torque
LQR	0.8225	5.8609×10^{-5}	4.809×10^{-4}
LBC	0.8069	5.8622×10^{-5}	4.849×10^{-4}
SMC	0.1229	6.1920×10^{-6}	4.0972×10^{-5}

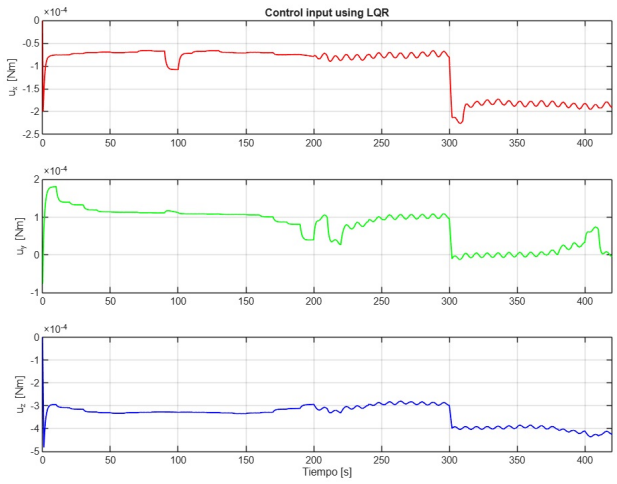

Fig. 6. LQR Control Effort

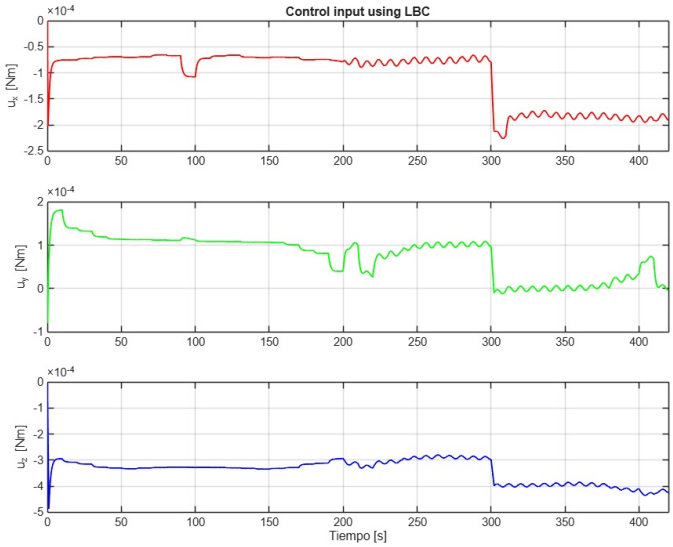

Fig. 7. LBC Control Effort

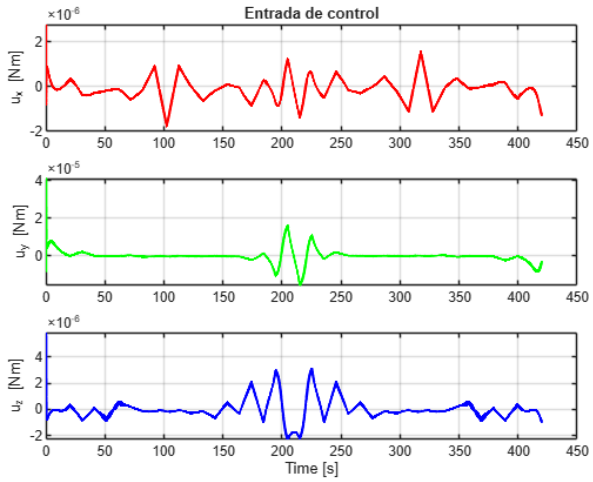

Fig. 8. SMC Control Effort

Discussion

The simulation results reveal clear performance differences among the evaluated attitude control strategies. While the linear quadratic regulator (LQR) and the Lyapunov-based controller achieve comparable attitude tracking behavior, the sliding mode controller (SMC) exhibits consistently superior tracking performance throughout the maneuver. This behavior can be attributed to the inherent robustness properties of sliding mode control, which explicitly account for model uncertainties and nonlinear dynamics through the enforcement of a predefined sliding manifold. Despite their different design approaches, both LQR and Lyapunov-based controllers show similar convergence characteristics, although the tuning process for the LQR required a more iterative procedure, as initial parameter selections did not yield satisfactory transient responses. In the case of the Lyapunov-based controller, actuator torque saturation led to oscillatory control behavior, which was mitigated by increasing the derivative gain at the expense of a longer settling time. The SMC, in contrast, achieves improved tracking accuracy while maintaining relatively low control effort for most of the maneuver, although the characteristic chattering phenomenon associated with sliding mode control is still observed. This effect remains limited and does not result in excessive actuator loading or persistent saturation. All three controllers demonstrate robustness against both periodic and impulsive disturbance torques; however, due to the limited control authority inherent to CubeSat platforms, sufficiently large disturbance peaks may still drive the actuators into saturation, potentially degrading tracking performance.

Conclusion

This paper presented a comparative study of three attitude control strategies for a CubeSat platform, namely a Lyapunov-based controller, a linear quadratic regulator (LQR), and a sliding mode controller (SMC). A nonlinear quaternion-based dynamic model was considered, and a linearized representation was employed for the LQR design. All controllers were evaluated under identical simulation conditions, including actuator saturation and external disturbance torques, in order to ensure a fair comparison.

Simulation results demonstrate that all control strategies are capable of stabilizing the spacecraft attitude and maintaining robustness against both periodic and impulsive disturbances. The Lyapunov-based and LQR controllers exhibited similar tracking performance, although the tuning of the LQR required a more iterative procedure and the Lyapunov controller showed sensitivity to actuator saturation, which influenced its transient response. Among the evaluated approaches, the sliding mode controller achieved the best overall performance, providing improved tracking accuracy and enhanced robustness while maintaining bounded control effort, despite the presence of mild chattering effects.

These findings suggest that sliding mode control represents a promising solution for CubeSat attitude control applications, particularly in scenarios involving nonlinear dynamics, external disturbances, and limited actuation capabilities.

Future work will focus on refining the SMC formulation to further reduce chattering, extending the analysis to more realistic orbital environments, and validating the proposed control strategies through hardware-in-the-loop simulations or experimental testing.

REFERENCES

[1] M. Helmy, A. T. Hafez, and M. Ashry, "CubeSat Reaction Wheels Attitude Control Via Modified PI-D Controller," in *Proc. 2022 International Telecommunications Conference (ITC-Egypt)*, 2022, pp. 1–6, doi: 10.1109/ITC-Egypt55520.2022.9855679.

[2] E. D. Cortés G., E. Rosero, and G. W. Rodriguez P., "Non-Linear Control Strategies for Attitude Maneuvers of a LEO CubeSat Based on Modified Rodrigues Parameters," in *Proc. 2023 IEEE 6th Colombian Conference on Automatic Control (CCAC)*, 2023, pp. 1–6, doi: 10.1109/CCAC58200.2023.10333817.

[3] J. Mamarasulov, J. Holaza, and M. Gulan, "Design of an MPC-Based Attitude Control System for a CubeSat Nanosatellite," in *Proc. 23rd International Conference on Process Control (PC)*, 2021, pp. 266–271, doi: 10.1109/PC52310.2021.9447494.

[4] A. M. Said, S. S. Michael, A. Magdy, O. Hisham, and M. Lotfy, "Simulation of CubeSat Attitude Control Subsystem Using B-Dot and PD Controllers," in *Proc. 7th Novel Intelligent and Leading Emerging Sciences Conference (NILES)*, 2025, pp. 390–395, doi: 10.1109/NILES68063.2025.11232219.

[5] M. Swartwout, "CubeSat Mission Assurance Trends," Presentation at the NEPP Electronics Technology Workshop, Saint Louis University, Parks College of Engineering, Aviation & Technology, Jun. 18, 2020. [Online]. Available: NEPP Electronics Technology Workshop.

[6] V. I. Utkin, *Sliding Modes in Control and Optimization*. Springer, 1992.

[7] J.-J. E. Slotine and W. Li, *Applied Nonlinear Control*. Prentice Hall, 1991.

[8] B. Wie, *Space Vehicle Dynamics and Control*. AIAA Education Series, 2008.